Journal of Experimental Botany, Vol. 62, No. 15, pp. 5595–5605, 2011
doi:10.1093/jxb/err243 Advance Access publication 23 August, 2011

Journal of Experimental Botany
www.jxb.oxfordjournals.org

RESEARCH PAPER

Characterization of a dual-affinity nitrate transporter MtNRT1.3 in the model legume *Medicago truncatula*

Marie-Christine Morère-Le Paven[1], Laure Viau[1], Alain Hamon[2], Céline Vandecasteele[3], Anthoni Pellizzaro[1], Céline Bourdin[2], Carole Laffont[4], Bruno Lapied[2], Marc Lepetit[5], Florian Frugier[4], Christian Legros[2] and Anis M. Limami[1,*]

[1] University of Angers, UMR-1191 Physiologie Moléculaire des Semences, IFR 149 Quasav, 2 Boulevard Lavoisier, 49045 Angers cedex 01, France
[2] University of Angers, Laboratoire RCIM, UPRES EA 2647, USC INRA 2023, IFR 149 Quasav, 2 Boulevard Lavoisier, 49045 Angers cedex 01, France
[3] INRA Angers, UMR-1191 Physiologie Moléculaire des Semences, IFR 149 Quasav, 16 Boulevard Lavoisier, 49045 Angers cedex 01, France
[4] Institut des Sciences du Végétal (ISV), Centre National de la Recherche Scientifique, 91198 Gif sur Yvette cedex, France
[5] Biochimie et Physiologie Moléculaire des Plantes, UMR 5004, INRA-CNRS-Sup Agro-UM2, Institut de Biologie Intégrative des Plantes, 34060 Montpellier, France

* To whom correspondence should be addressed. E-mail: anis.limami@univ-angers.fr

Received 6 April 2011; Revised 15 July 2011; Accepted 18 July 2011

Abstract

Primary root growth in the absence or presence of exogenous NO_3^- was studied by a quantitative genetic approach in a recombinant inbred line (RIL) population of *Medicago truncatula*. A quantitative trait locus (QTL) on chromosome 5 appeared to be particularly relevant because it was seen in both N-free medium (LOD score 5.7; R^2=13.7) and medium supplied with NO_3^- (LOD score, 9.5; R^2=21.1) which indicates that it would be independent of the general nutritional status. Due to its localization exactly at the peak of this QTL, the putative NRT1-NO_3^- transporter (*Medtr5g093170.1*), closely related to *Arabidopsis* AtNRT1.3, a putative low-affinity nitrate transporter, appeared to be a significant candidate involved in the control of primary root growth and NO_3^- sensing. Functional characterization in *Xenopus* oocytes using both electrophysiological and $^{15}NO_3^-$ uptake approaches showed that *Medtr5g093170.1*, named *MtNRT1.3*, encodes a dual-affinity NO_3^- transporter similar to the AtNRT1.1 'transceptor' in *Arabidopsis*. *MtNRT1.3* expression is developmentally regulated in roots, with increasing expression after completion of germination in N-free medium. In contrast to members of the NRT1 superfamily characterized so far, *MtNRT1.3* is environmentally up-regulated by the absence of NO_3^- and down-regulated by the addition of the ion to the roots. Split-root experiments showed that the increased expression stimulated by the absence of NO_3^- was not the result of a systemic signalling of plant N status. The results suggest that MtNRT1.3 is involved in the response to N limitation, which increases the ability of the plant to acquire NO_3^- under N-limiting conditions.

Key words: *Medicago truncatula*, nitrate transport, NO_3^-, NRT1, primary root growth, QTL.

Introduction

Nitrogen (N) is an essential element for all plants. Higher herbaceous plants obtain the majority of their N from the assimilation of nitrate and subsequent reduction to ammonium. The first step of the nitrate assimilation pathway is the entry of nitrate into the cell, a process that is mediated by specific transporters. Based on their kinetics, nitrate uptake systems have been classified into two groups: the low-affinity transport system (LATS) and the high-affinity

Abbreviations: HATS, high-affinity transport system; LATS, low-affinity transport system; QTL, quantitative trait locus; RIL, recombinant inbred line.

transport system (HATS). The LATS operates at high external nitrate concentrations and shows no evidence of saturation *in planta*, even at NO_3^- concentrations as high as 50 mM. The HATS (K_m <200 μM) operates at low external nitrate concentration, and has inducible (iHATS) and constitutive (cHATS) components (Siddiqi *et al.*, 1989, 1990; Glass *et al.*, 1992). Three plant gene families encode nitrate carrier proteins: the large PTR family (51 members in *Arabidopsis*), including the NRT1 and NAXT proteins (Segonzac *et al.*, 2007), the NRT2 family, encoding HATS components (Miller *et al.*, 2007), and the CLC family (Zifarelli and Pusch, 2010). NRT1 proteins have been identified in several species, for example *Arabidopsis thaliana*, *Brassica napus*, and *Oryza sativa* (for reviews, see Forde, 2000; Miller *et al.*, 2007; Tsay *et al.*, 2007). Compared with the large number of genes in these families, only a few members were functionally characterized as NO_3^- transporters based on heterologous systems, for example in *Arabidopsis* AtNRT1.1, AtNRT1.2 (Tsay *et al.*, 1993; Huang *et al.*, 1999), AtNRT1.4 (Chiu *et al.*, 2004), AtNRT1.5 (Lin *et al.*, 2008), and AtNRT1.6 (Almagro *et al.*, 2008), in rice OsNRT1 (Lin *et al.*, 2000), and in *B. napus* BnNRT1.2 (Zhou *et al.*, 1998).

The most studied NRT1 transporter is the *Arabidopsis* AtNRT1.1 protein (originally named CHL1). Its expression is inducible by nitrate (Huang *et al.*, 1996), and functional characterization in *Xenopus* oocytes revealed its involvement in low- as well as high-affinity nitrate uptake, behaving both as a LATS and HATS component. This transporter is therefore currently considered as a dual-affinity nitrate transporter (Wang *et al.*, 1998; Liu *et al.*, 1999). *AtNRT1.1* expression is also developmentally regulated, being mainly expressed in nascent organs, stems, leaves, flower buds, and roots (Guo *et al.*, 2001). AtNRT1.1 was functionally linked to the stimulatory effect of nitrate on root growth (Walch-Liu *et al.*, 2006; Walch-Liu and Forde, 2008). AtNRT1.1 has been shown to play a role in the nitrate-sensing system that stimulates root growth in nitrate-rich patches by promoting auxin fluxes in root apices (Ho *et al.*, 2009; Krouk *et al.*, 2010).

Nitrate transporters in legumes to date have received little interest, probably because these species are able to adapt to N starvation by promoting a specific response: the biological N_2 fixation in symbiotic nodules (Crespi and Frugier, 2008). Consequently, although nitrate also plays important nutritional and signalling roles in legumes, only few putative nitrate transporters were cloned in these species (Yokoyama *et al.*, 2001) and none of them has been functionally characterized so far. Indeed, under N-limited conditions, legumes absorb mineral N and particularly NO_3^- to fulfil their nutritional demand before functional symbiotic nodules are differentiated. In addition, nitrate is known to repress nodulation and N_2 fixation activity (Streeter, 1985*a*, *b*; Barbulova *et al.*, 2007), involving both local and systemic regulatory pathways (Jeudy *et al.*, 2010). N supply was shown to modulate nodule initiation in *Lotus japonicus* by predisposing plants to successful or unsuccessful interactions with rhizobia prior to inoculation (Omrane *et al.*, 2009). The inhibitory effect of high exogenous N concentrations on the competence of plants to nodulate was maintained several days after transfer to low N concentration (Omrane *et al.*, 2009).

Whether NO_3^- repressive effects are due to the ion itself, to products of its assimilation, or both is not yet clearly demonstrated. Receptor-like kinases acting in legume shoots, *HAR1* (Hypernodulation and Aberrant Roots) in *L. japonicus*, *SUNN* (Supernumerous Nodules) in *Medicago truncatula*, *SYM29* (Symbiosis29) in pea, and *NARK* (Nodule Autoregulation Receptor Kinase) in soybean (Krusell *et al.*, 2002; Nishimura *et al.*, 2002; Searle *et al.*, 2003; Schnabel *et al.*, 2005), are involved in nitrate inhibition of nodulation (Okamoto *et al.*, 2009).

Recent findings suggest that a protein belonging to the NRT1(PTR) family, encoded by the *M. truncatula LATD/NIP* gene (lateral root organ defective/numerous infections and polyphenolics), regulates the legume root system architecture. *LATD/NIP* is expressed in the root apical meristem and elongation zones, as well as in the nodule meristem and infection zones (Liang *et al.*, 2007; Yendrek *et al.*, 2010). Accordingly, LATD/NIP is required for the establishment and maintenance of primary root, lateral root, and symbiotic nodule meristems (Yendrek *et al.*, 2010). In addition, the *latd* mutant is not sensitive to the inhibition of primary root growth by nitrate.

In the present work, the first functional characterization of an *M. truncatula* nitrate transporter, MtNRT1.3, is reported. This transporter behaves as a dual-affinity nitrate transporter when expressed in *Xenopus* oocytes. Interestingly, unlike members of the NRT1 superfamily characterized so far, in roots the expression of *MtNRT1.3* is locally stimulated by N starvation and repressed in medium supplied with NO_3^-. The present data suggest that this transporter probably does not have a major role in overall root NO_3^- acquisition but may rather be involved in the plant response to NO_3^- starvation.

Materials and methods

Seed germination and seedling growth conditions

The *M. truncatula* lines used in this study were Jemalong-6 (reference line for genomic data named A17) and DZA315.16. Seeds were scarified with glass paper, and 40 seeds per Petri dish were imbibed with 5 ml of de-ionized water on sterilized paper, stored for 5 h at 21 °C, and for 4 d at 4 °C in the dark in order to break dormancy.

For expression analysis of *MtNRT1.3* in radicles and primary roots in the absence of nitrate, seeds germinated in Petri dishes were maintained in darkness in a growth chamber at 21 °C and samples (radicles and primary roots) were collected after 24, 48, 96, and 120 h of imbibition.

For expression analysis of *MtNRT1.3* in roots in the presence or absence of nitrate, germinated seeds were transferred after 48 h of imbibition either on N-free medium or on medium supplied with N (KNO_3 5 mM) with a 16 h/8 h light/dark regime. The compositions of the nutrient solutions were as described previously (Richard-Molard *et al.*, 1999). Systemic regulation of *MtNRT1.3* expression by nitrate was carried out in roots of plants growing in a split-root system as described in Ruffel *et al.* (2008). The

expression of *MtNRT1.3* was also studied in nodules of plants grown *in vitro* for 7 d on an N-deprived medium, 'I' medium (Gonzalez-Rizzo *et al.*, 2006), and spot-inoculated with a *Sinorhizobium meliloti* Sm1021 strain ($OD_{600\ nm}$=0.05, 0.4% agar). Root segments or nodules were collected at the indicated time points: 1 day post-inoculation (dpi; dividing cortical cells stage), 3 dpi (nodule primordium stage), and 8 dpi (young N_2-fixing nodule stage).

In all experiments, harvested samples were immediately frozen in liquid nitrogen and stored at –80 °C.

Phenotyping and quantitative trait locus (QTL) analysis

A population of 171 recombinant inbred lines (RILs), named LR4, was derived from a cross between A17 and DZA315.16 (Pierre *et al.*, 2008). After scarification with glass paper, seeds were imbibed on filter paper in 12 cm square transparent plates containing either N-free medium or medium supplied with N (KNO_3 5 mM). After 5 h at 21 °C and 96 h at 4 °C in the dark, plates were placed at a 45 ° angle at 20 °C with a 16 h photoperiod under a light intensity of 200 µmol m^{-2} s^{-1}. Plates were randomized following a complete-block design with two blocks, each containing one plate with 10 seedlings per line for each treatment. Primary root length, determined 168 h after imbibition, was scored by marking the plate covers, and corresponding images were analysed using ImageJ software (http://rsbweb.nih.gov/ij/). All statistical analyses were performed with the SAS 8.1 software (SAS Institute, 2000).

A genetic map was built by Vandecasteele *et al.* (2011) with MTE markers anchored on the physical map (Huguet *et al.*, 2007). QTL mapping was carried out using MCQTL software (Jourjon *et al.*, 2005) with the iterative QTL mapping method (iQTL). Cofactors were selected by forward regression using an *F*-test for a global genome-wide type I risk of 10%. The *F* threshold for QTL detection was automatically determined for all traits by 1000 iterations of permutation tests at a global genome-wide type I risk of 5%. For each QTL identified, additive genetic effect, percentage of phenotypic variance explained (R^2), *F*-test value, as well as the confidence interval were determined by the MCQTL software. Equivalent LOD scores were then calculated.

RNA extraction and reverse transcription

Total RNA was extracted from tissues ground in liquid nitrogen using TriReagent (Ambion, Austin, TX, USA), following the manufacturer's instructions. Samples were further purified using NucleoSpin RNA clean-up (Macherey-Nagel, Düren, Germany). RNAs were quantified using an ND-1000 spectrophotometer (Nanodrop, Wilmington, DE, USA) and 2 µg were checked on a 1% agarose gel to ensure their integrity.

cDNA syntheses were performed with 2 µg of total RNAs with the MMLV reverse transcriptase (Promega, Madison, Wisconsin, USA) or the Supercript II reverse transcriptase (Invitrogen, Carlsbad, CA, USA), following the manufacturers recommendations.

Real-time reverse transcription-PCR (RT-PCR)

Primers were designed using the Primer-Express software (Applied Biosystems, Forster City, CA, USA) (Table 1).

Reactions were performed in triplicate using the SYBR Green ready Master mix (Applied Biosystems) on an ABI Prism 7000 sequence detection system (Applied Biosystems), or alternatively on a LightCycler480 with appropriate reagents (Roche, Switzerland). To check for specificity, a dissociation curve was analysed for each run as well as the sequencing of the amplicon. An efficiency threshold of 90% was used (T_m=60 °C; primers indicated in Table 1). mRNA amounts were calculated and the results were expressed as a the ratio of the *MtNRT1.3* gene to endogenous references (indicated in the figure legends).

Table 1. Primers used for real-time RT-PCR

Sequence name	Oligonucleotide sequence (5′ to 3′)
MtNRT1.3	Fwd: CAGGTCCCTTGACAAAGCAGCAATC
	Rev: GCATGTTGACCAAATGGGAAGGAG
18S rDNA	Fwd: GAAACGGCTACCACATCCAAG
	Rev: AGCCCGGTATTGTTATTTATTGTC
MtRBP1	Fwd: AGGGGCAAGTTCCTTCATTT
	Rev: GGTAGAAGTGCTGGCTCAGG

Fwd, forward primer; Rev, reverse primer.

Amplification of the MtNRT1.3 *open reading frame*

The *MtNRT1.3* open reading frame was amplified by RT-PCR in the A17 or DZA315.16 genotypes using the following primer pair, 5′-ATGGTTCTTGTTGCAAGCAA-3′ and 5′-ATGGGAAGGAAGAAGTATAG-3′, and the *Pfu* DNA polymerase (Promega). Reactions were carried out in an Icycler (Bio-Rad, Marne-La-Coquette, France) with a standard protocol (T_m=54 °C). PCR fragments were modified using an A-tailing procedure (GoTaq, Promega) and subsequently cloned into a PGEM-T easy vector (Promega).

Functional analysis of MtNRT1.3 in Xenopus *oocytes*

The *MtNRT1.3* open reading frame was subcloned into the *Xenopus* expression vector pGEM-HEJUEL (Shih *et al.*, 1998). The vector contains the 5′- and 3′-untranslated regions of the *Xenopus* β-globin gene flanking a multiple cloning site. The recombinant plasmid was linearized with *Stu*I, and capped mRNA was transcribed *in vitro* using the mMESSAGE mMACHINE kit (Ambion). Ovarian lobes were surgically harvested from adult *Xenopus laevis* females and washed in a standard oocyte saline (SOS) buffer composed of (in mM): NaCl 100, KCl 2, $CaCl_2$ 1.8, $MgCl_2$ 1, HEPES 5, pH 7.5. Stage V–VI oocytes were defolliculated manually using fine forceps after treatment for 10–15 min with 2 mg ml^{-1} collagenase (type 1A, Sigma-Aldrich, Saint Quentin Fallavier, France) in calcium-free SOS. Defolliculated oocytes were injected with 40 ng of complementary RNA (cRNA) and stored in a sterile medium composed of SOS supplemented with gentamycin (50 µg ml^{-1}), penicillin (100 U ml^{-1}), streptomycin (100 µg ml^{-1}), sodium pyruvate (2.5 mM), and horse serum (1–5%). Two days after injection, oocytes were tested for *MtNRT1.3* expression using 3 M KCl-filled borosilicate electrodes connected to a two-electrode voltage-clamp amplifier (GeneClamp 500; Axon Instruments, Foster City, CA, USA). Each cell was clamped at a holding potential of –60 mV and equilibrated for 5 min with a solution containing 230 mM mannitol, 0.15 mM $CaCl_2$, and 10 mM HEPES, pH 5.5. Nitrate transport activity was then induced using a bath solution containing 220 mM mannitol, 0.15 mM $CaCl_2$, 10 mM HNO_3, and 10 mM HEPES (pH 5.5). Exposure to nitrate was maintained for <1 min to minimize the accumulation of ions within the cell. Steady-state current–voltage (I–V) relationships were obtained by eliciting voltage steps of 300 ms duration using 20 mV increments from the holding potential (–60 mV), to reach various potentials ranging from –20 mV to –180 mV. Steady-state currents were measured at the end of the 300 ms test pulses. Nitrate-elicited currents were obtained by subtracting currents measured before treatment from those obtained after addition of nitrate. Recording and analysis were performed with the pClamp8 software (Axon Instruments).

For uptake assays using [^{15}N]nitrate, batches of 10 injected oocytes were incubated in a 200 µl solution containing 230 mM mannitol, 0.3 mM $CaCl_2$, 10 mM MES-TRIS pH 5.5, and different concentrations of $^{15}NO_3$ (ranging from 25 µM to 400 µM for the kinetic study and at 250 µM or 10 mM for high-affinity or low-affinity

uptake assays, respectively) supplied as $K^{15}NO_3$ for 3–12 h at 18 °C. Oocytes were then rinsed five times with a cold nitrate-free SOS solution, individually dried at 60 °C for almost 24 h, and the retained ^{15}N was determined on a continuous flow using a C/N analyser linked to an isotope ratio mass spectrometer (IRMS, EA3000, EuroVector, Milan, Italy) coupled to a mass spectrometer (IsoPrime, Elementar, Hanau, Germany). Oocytes injected with the *AtNRT1.1* (*CHL1*) cRNA (Liu *et al.*, 1999) were used as a positive control.

Results

Detection, cloning, mapping, and in silico *analysis of* Medtr5g093170.1 *(*MtNRT1.3*), a gene encoding a putative nitrate transporter*

Medicago truncatula lines Jemalong-6 (A17) and DZA315.16 were tested for primary root growth and sensitivity to exogenous NO_3^-. DZA315.16 primary root growth showed a higher sensitivity to the NO_3^- inhibitory effect than A17. Based on these parental differences, the variability in primary root growth was assessed on a population of 171 RILs derived from the cross between A17 and DZA315.16. A strong reduction in primary root growth was observed in medium supplied with NO_3^- among the RIL population (Fig. 1). The average length of the primary root after 168 h among the RIL population was 59.9 mm in the N-free medium while it decreased significantly (P <0.0001) to 50.5 mm in the medium supplied with NO_3^- (Fig. 1). Several QTLs involved in the control of primary root growth were detected (Table 2). Specific attention was drawn to an NRT1-like putative NO_3^- transporter, *Medtr5g093170.1*, located within the confidence interval of a major QTL on chromosome 5 (http://www.medicago.org/genome/), revealed in both N-free medium and medium supplied with NO_3^-. The *Medtr5g093170.1* open reading frame was amplified by PCR in both parental lines (Genbank accession no. GU966590; Fig. 2). The detected polymorphism between the two alleles was used to map the gene and confirmed its localization on chromosome 5 (87.5 cM). Furthermore it coincided exactly with the peak of the QTL (Fig. 3 and Table 2).

Sequence analysis revealed a 1767 bp open reading frame encoding a 588 amino acid protein (64.8 kDa), and phylogenetic analysis established that this protein is closely related to *Arabidopsis* and rice members of the NRT1 family (Fig. 4). The *M. truncatula* protein belongs to the NRT1(PTR) group I (Tsay *et al.*, 2007) and shares 49% identity with AtNRT1.1 and 70% identity with AtNRT1.3; therefore, it was named MtNRT1.3. Like all other members of the NRT1 family, the MtNRT1.3 protein is predicted to contain 12 putative transmembrane (TM) domains with a long hydrophilic loop between TMs 6 and 7 (Fig. 2). Two

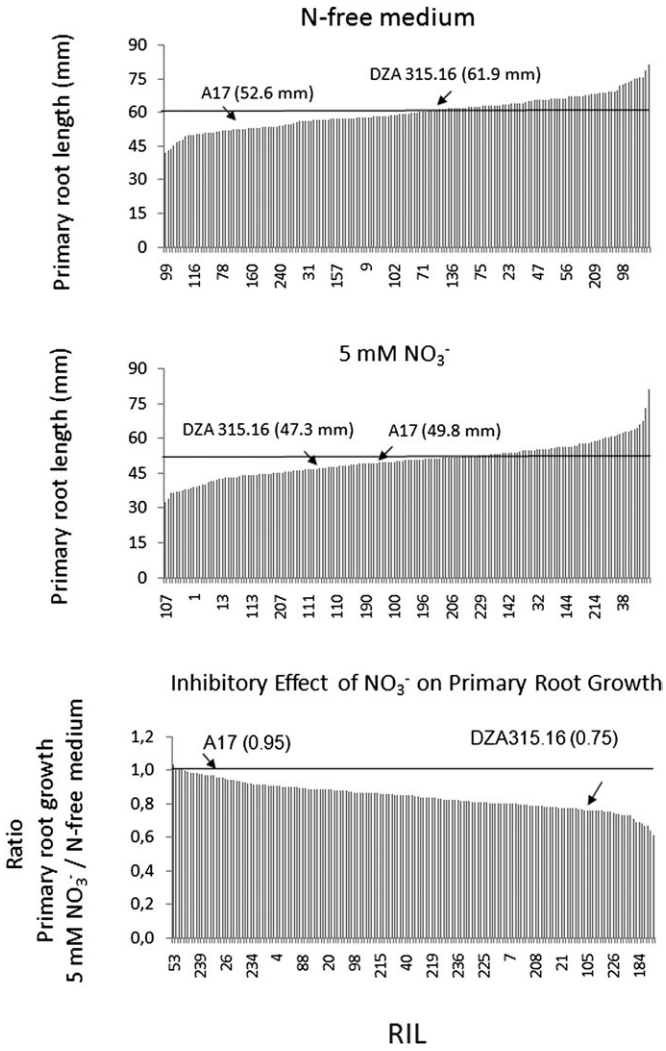

Fig. 1. Phenotyping of the LR4 recombinant inbred line (RIL) population, derived from the cross between A17 and DZA315.16. Primary root length was determined after 168 h of imbibition on N-free medium or on medium containing 5 mM KNO_3. The nitrate inhibitory effect on primary root growth is expressed as a ratio: primary root growth on nitrate-supplied medium/primary root growth on N-free medium. Arrows indicate the positions of both parents.

Table 2. M. truncatula *QTLs for primary root growth.*

Trait	Chromosome	Location (cM)	Confidence interval (cM)	LOD	R^2 (%)	A17 effect
Primary root growth (N-free medium)	5	41.9	31.5–72.7	3.4	8.8	–2.26
	5	87.5	69.6–90.9	5.7	13.7	–2.57
Primary root growth (5 mM NO_3^-)	1	23.5	10.3–60.6	2.9	7.6	+2.08
	5	87.5	77.4 90.2	9.5	21.1	–3.22
	7	56.7	45.9–67.4	3.4	8.7	–2.08

QTLs were identified on N-free or on nitrate (KNO_3 5 mM) media, and revealed by composite interval mapping in recombinant inbred lines of the LR4 population (Pierre *et al.*, 2008).

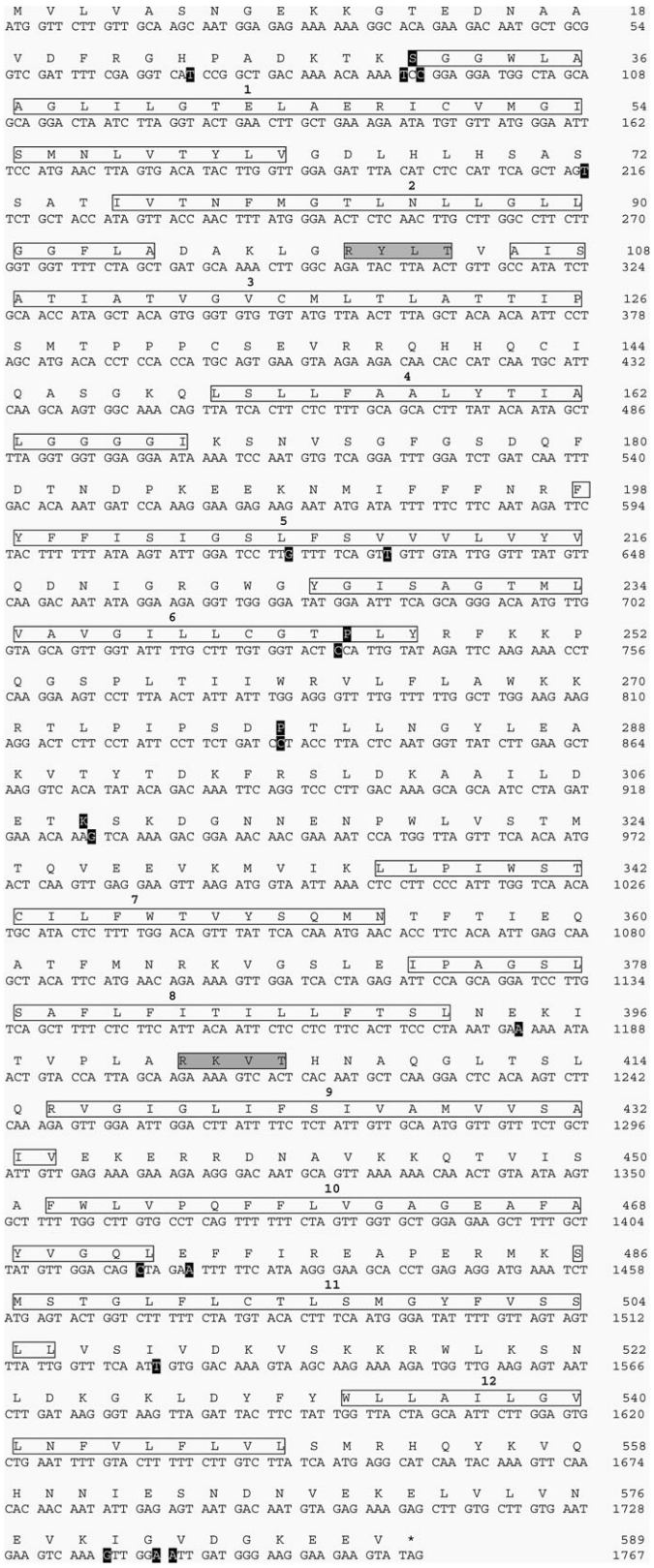

Fig. 2. Sequence of *Medtr5g093170.1* (*MtNRT1.3*) of A17. The nucleotide sequence of *MtNRT1.3* (accession no. GU966590) and the deduced amino acid sequence of the MtNRT1.3 protein are presented. The putative transmembrane regions are enclosed in boxes and numbered (http://www.ch.embnet.org/). The putative phosphorylation sites are boxed and shaded. The 16 bases and four amino acids differing in DZA315.16 are indicated in black.

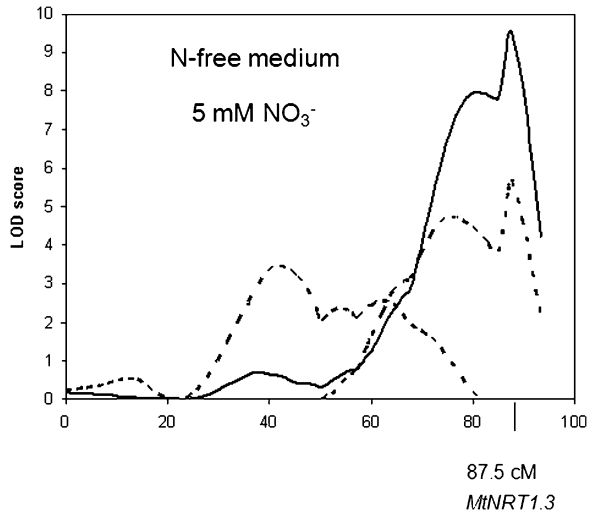

Fig. 3. QTL likelihood plots indicating LOD scores for primary root growth on N-free medium or medium supplied with 5 mM KNO_3 along chromosome 5.

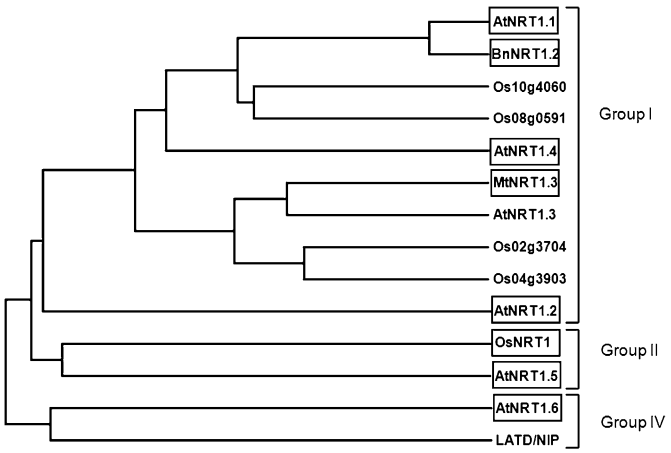

Fig. 4. Phylogenetic tree of MtNRT1.3 and its homologues in different plant species. The phylogram was created using Tree-Top-Phylogenetic Tree Prediction (http://www.genebee.msu.su/index.html). AtNRT1.1, AtNRT1.2, AtNRT1.4, AtNRT1.5, and AtNRT1.6 are nitrate transporters from *A. thaliana* (Tsay *et al.*, 1993; Huang *et al.*, 1999; Chiu *et al.*, 2004; Almagro *et al.* 2008; Lin *et al.* 2008), BnNRT1.2 is a nitrate/His transporter of *Brassica napus* (Zhou *et al.*, 1998), and OsNRT1 is a nitrate transporter of *Oryza sativa* (Lin *et al.*, 2000). All the above-mentioned proteins are boxed. Other proteins of *A. thaliana* (AtNRT1.3), of *O. sativa* (Os10g4060, Os08g0591, Os02g3704, Os04g3903), and of *M. truncatula* (LATD/NIP) belong to the NRT1(PTR) family but have not been proven to encode nitrate transporters (Tsay *et al.*, 2007; Yendrek *et al.*, 2010).

putative phosphorylation sites (RXXT/S) are predicted at positions T^{104} and T^{405}. Sequence alignment indicated that $RXXT^{104}$ is identical to the phosphorylable site present at position $RXXT^{101}$ in the AtNRT1.1 protein (Liu and Tsay, 2003). The comparison of parental sequences showed a polymorphism affecting 16 bases and four amino acids: S_{31}-T, P_{245}-S, P_{279}-H, and K_{309}-N.

Functional characterization of the putative nitrate transporter MtNRT1.3 *in* Xenopus *oocytes*

The *Xenopus* oocyte expression system was used to investigate whether the protein encoded by *MtNRT1.3* is an NO_3^- transporter. *In vitro* synthesized *MtNRT1.3* cRNAs were microinjected into *Xenopus* oocytes. Two days after injection oocytes were assessed for nitrate transport activity at pH 5.5. Millimolar concentrations of nitrate induced inward currents that increased with hyperpolarization in oocytes injected with MtNRT1.3 cRNAs, whereas no current could be recorded from water-injected control oocytes (Fig. 5A). Kinetic analysis of currents elicited by different NO_3^- concentrations in the low-affinity range (5–30 mM) in three independent experiments (using at least 10 injected oocytes) showed saturable LATS kinetics (data not shown), indicating that *MtNRT1.3* encodes a low-affinity nitrate transporter. In order to determine accurately the K_m of MtNRT1.3 for its substrate, *MtNRT1.3*-injected oocytes were incubated with $^{15}NO_3^-$ in millimolar concentrations. Kinetic analysis of ^{15}N enrichment in oocytes incubated in different NO_3^- concentrations ranging from 1 mM to 30 mM showed saturable low-affinity kinetics with a K_m of 7.2 mM (Fig. 5B). To date, among the nitrate transporters functionally characterized in heterologous systems, AtNRT1.1 was the only dual-affinity nitrate transporter (Liu *et al.*, 1999). MtNRT1.3 activity was also tested at low NO_3^- concentrations. Kinetic analysis of ^{15}N enrichment in oocytes incubated in different NO_3^- concentrations ranging from 25 μM to 400 μM showed saturable high affinity kinetics with a K_m of 41.6 μM (Fig. 5B). This result indicates that MtNRT1.3 also corresponds to a high-affinity

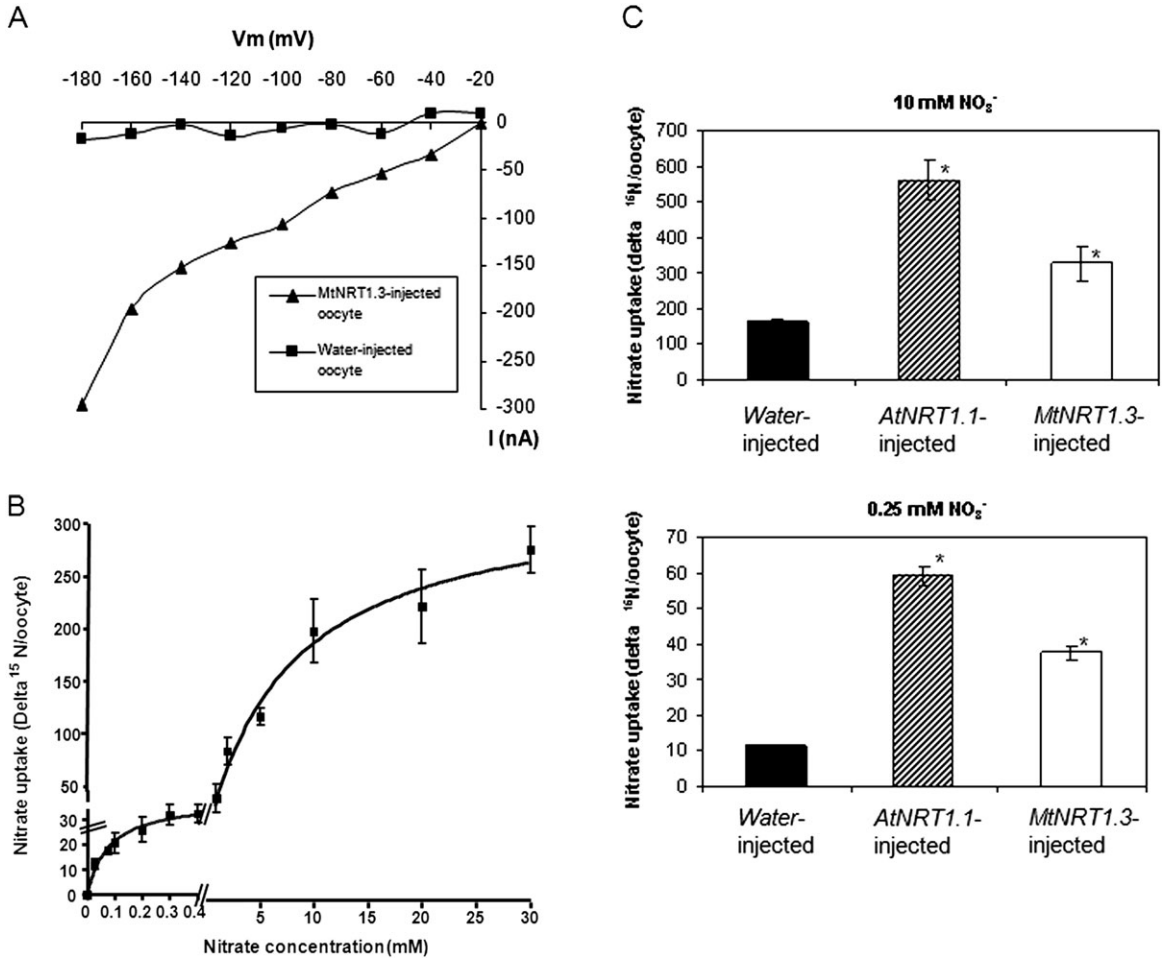

Fig. 5. (A) Electrophysiological analyses: voltage dependence of nitrate-elicited currents in *Xenopus* oocytes injected with *MtNRT1.3*. Currents were obtained by the difference between measurements conducted in the presence and absence of 30 mM nitrate at pH 5.5. Current amplitudes were measured at the end of 300 ms rectangular test pulses (Vhold= –60 mV, Vtest= –20 mV to –180 mV). Control (water-injected) oocytes were treated under the same conditions. Similar results were obtained with three other batches of oocytes isolated from different frogs. (B) Kinetic analysis of nitrate uptake in *MtNRT1.3*-injected oocytes in the high- and low-affinity concentration range. *MtNRT1.3*-injected oocytes were incubated with $^{15}NO_3^-$ concentrations from 25 μM to 400 μM and from 1 m to 30 mM at pH 5.5. Oocytes were individually dried and the retained ^{15}N was measured by mass spectrometry. Each data point is the mean ±SE for 8–10 oocytes. (C) Nitrate uptake comparison between *MtNRT1.3*- and *AtNRT1.1*-injected oocytes. In both cases, oocytes were incubated with 10 mM or 0.25 mM $^{15}NO_3^-$ at pH 5.5. Each data point is the mean ±SE for 8–10 oocytes. *Significantly different when compared with the water-injected control (Breusch-Pagan test, α=0.01).

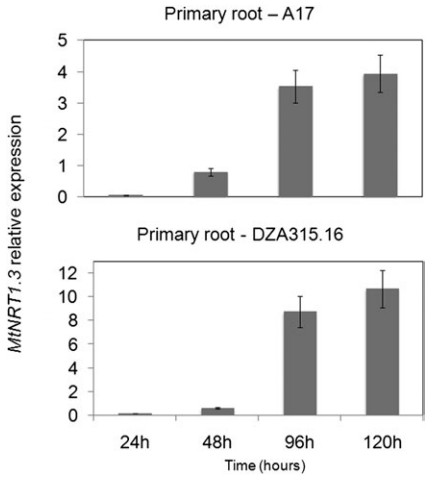

Fig. 6. *MtNRT1.3* expression determined by quantitative RT-PCR in primary roots of *M. truncatula* after 24, 48, 96, and 120 h imbibition on de-ionized water. Error bars represent the standard deviation (P <0.001) of three technical replicates and three independent biological replicates.

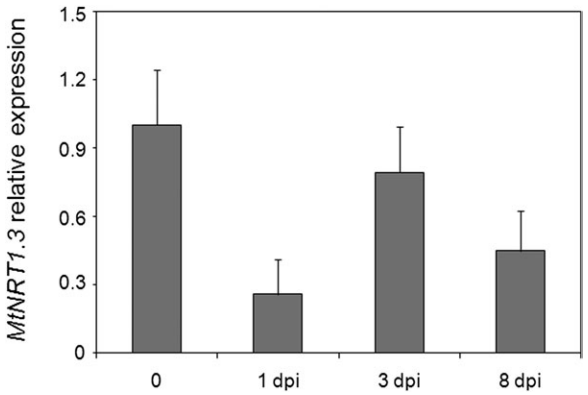

Fig. 7. Expression of *MtNRT1.3* in the kinetics of symbiotic nodulation under N starvation. One day post-inoculation (dpi) corresponds to dividing cortical cells and early rhizobial epidermal infection; 3 dpi corresponds to nodule primordial; and 8 dpi corresponds to N_2-fixing mature nodules. Error bars represent the standard deviation (P <0.001) of two biological experiments with two technical replicates (cDNA derived from the same RNA).

nitrate transporter. As a positive control, oocytes of the same batch were injected with *AtNRT1.1* and *MtNRT1.3*. As expected, a dual-affinity nitrate uptake activity was detected for AtNRT1.1 (Fig. 5C) (Liu *et al.*, 1999). Collectively, the results indicate that the MtNRT1.3 protein is a dual-affinity nitrate transporter.

Developmental and environmental regulation of the dual-affinity nitrate transporter gene MtNRT1.3

Expression of *MtNRT1.3* was studied using real-time RT-PCR in primary roots of the two *M. truncatula* lines A17 and DZA315.16 that have never been submitted to nitrate. *MtNRT1.3* could not be detected in radicles at early stages of germination (24 h of imbibition); afterwards its expression increased in primary roots of both lines (Fig. 6). Under symbiotic conditions, expression of *MtNRT1.3* in N_2-fixing nodules was slightly lower than in roots grown without nitrate (Fig. 7).

The response of *MtNRT1.3* to nitrate was then studied in roots of germinated seedlings grown for 48 h on an N-free medium and transferred to a medium supplied with 5 mM KNO_3 for 5 h or 24 h. Expression of *MtNRT1.3* decreased by 37% and 54%, respectively, 5 h and 24 h after transfer of the seedlings to the medium supplied with NO_3^- (Fig. 8).

Systemic and local effects of NO_3^- on *MtNRT1.3* expression were also studied using plants growning in a split-root system as described in Ruffel *et al.* (2008). Hydroponically grown plants fed with 1 mM NO_3^- were subjected for 4 d to two N regimes. In control plants, 1 mM NO_3^- was maintained on both sides of the root system (CNO_3^- root). In treated plants, the N source was removed to the treated side of the root system ($-NO_3^-$ root). N starvation of the treated side of the root system lowered the N status of the plants (Ruffel *et al.*, 2008) as if the plants were growing under N-limiting conditions compared with the control. Therefore, the untreated roots of these plants were named LNO_3^- root (Fig. 9). *MtNRT1.3* expression was four times higher in $-NO_3^-$ root compared with LNO_3^- root. Comparison between the untreated roots of N-limited plants and the roots of control plants (LNO_3^- root versus CNO_3^- root) showed similar levels of *MtNRT1.3* expression.

Discussion

Primary root growth is an important trait for efficient rhizosphere colonization and successful seedling installation (Limami *et al.*, 2002; Glevarec *et al.*, 2004). In N-deprived soils, inorganic N fertilization is an important issue for legumes during early post-germination stages of development (i.e. before symbiotic nodulation and N_2 fixation occurs). However while NO_3^- is generally used as a starter-fertilizer to boost legume growth before nodulation, paradoxically exogenous NO_3^- has been shown to inhibit primary root growth in *M. truncatula* (Yendrek *et al.*, 2010). In the present work, a quantitative genetic approach was used to study primary root growth and the sensitivity of this trait to exogenous NO_3^- in a RIL population of *M. truncatula* derived from two contrasted parental lines, DZA315.16 and A17. DZA315.16 is characterized by a faster primary root growth in N-free medium and a higher sensitivity to NO_3^- than A17. Among the QTLs involved in the control of primary root growth, one located on chromosome 5 was very relevant due to its high LOD and R^2 scores, and because it was detected in both N-free and N-containing media, suggesting its independence from the nutritional status of the plant. Interestingly, a putative NRT1-NO_3^- transporter, localized exactly at the peak of this QTL, appeared to be a significant candidate to be involved in the control of primary root growth and NO_3^- sensing, and was therefore selected for functional characterization.

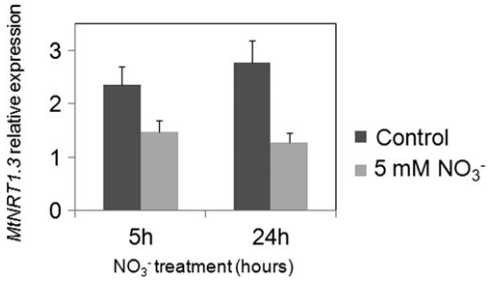

Fig. 8. *MtNRT1.3* expression determined by quantitative RT-PCR in primary root of *M. truncatula* after 5 h or 24 h of KNO_3 treatment. Error bars represent the standard deviation (P <0.001) of three technical replicates and three independent biological replicates.

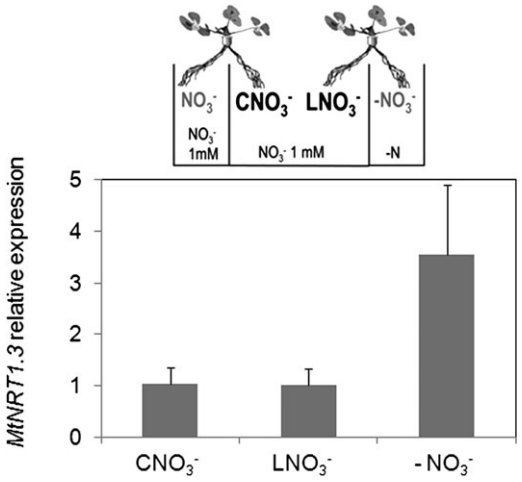

Fig. 9. *MtNRT1.3* expression determined by quantitative RT-PCR in roots of plants grown in a split-root system. Hydroponically grown plants fed with 1 mM KNO_3 were subjected for 4 d to two N regimes. In control plants, this same regime was maintained on both sides of the root system (CNO_3^-). In L plants (N-limited plants), the N source was removed to the treated side of the root system ($-NO_3^-$) and maintained in the other side (LNO_3^- roots). C and L roots were continuously exposed to the same local environment before and during the treatment. Error bars represent the standard deviation (P <0.001) of three technical replicates and three independent biological replicates.

Functional characterization of MtNRT1.3 in Xenopus *oocytes*

MtNRT1.3 was functionally characterized in *Xenopus* oocytes as a dual-affinity nitrate transporter. This transporter belongs to the family of NRT1 transporters. Only few plant *NRT1/PTR* genes have been proven to encode NO_3^- transporters, and all those tested to date were low-affinity nitrate transporters (LATS activity) except AtNRT1.1 (CHL1) that behaves as a dual-affinity nitrate transporter. Electrophysiological and $^{15}NO_3$ uptake experiments with nitrate concentrations in the range of 25–400 μM and 1–30 mM at pH 5.5 in oocytes injected with cRNA of *MtNRT1.3* revealed saturable kinetics with K_m values of 41.6 μM and 7.2 mM. Taken together, these data indicated that MtNRT1.3 contributes to LATS and HATS activities, similarly to AtNRT1.1 in *Arabidopsis*.

Sequence comparison of MtNRT1.3 revealed that the closest *Arabidopsis* homologue is AtNRT1.3 that is a putative low-affinity nitrate transporter. Nevertheless, the phosphorylation site $RXXT^{101}$ responsible for the shift between low and high affinity in AtNRT1.1 is conserved in MtNRT1.3. This sequence is, however, also found in low-affinity nitrate transporters, indicating that additional sequences are needed for the dual affinity switch (Tsay *et al.*, 2007).

Regulation of MtNRT1.3 *expression*

MtNRT1.3 was not expressed in radicles of *M. truncatula* at the onset of germination (24 h of imbibition) but its expression was detected in primary roots of seedlings, in the absence of NO_3^- in the external medium as early as 2 d after completion of germination. Furthermore, *MtNRT1.3* transcripts decreased upon exposure to NO_3^-, suggesting an inhibitory effect of NO_3^- (or a compound derived from its assimilation). Interestingly, this profile of expression is in contrast to the mode of regulation of all the NRT1 proteins functionally characterized so far as NO_3^- transporters. Indeed, only NO_3^--inducible (e.g. *LeNRT1.2* and *AtNRT1.1*) or constitutively expressed (e.g. *AtNRT1.2*, *LeNRT1.1*, and *OsNRT1*) transporters were described previously (see the Introduction). Further characterization of the expression of *MtNRT1.3* was carried out in plants growing in a split-root system. In N-limited plants the expression of *MtNRT1.3* increased in the root side transferred to the N-free nutrient solution ($-NO_3^-$ root) while it remained unchanged in the root side that remains in 1 mM NO_3^- nutrient solution (LNO_3^- root) and at a similar level to that in CNO_3^- root of control plants. These results indicate that the stimulation of gene expression was driven by the absence of the ion and that it was not the result of a systemic signal triggered by whole plant N limitation, such as the release of feedback limitation by downstream N metabolites. These results suggest the involvement of *MtNRT1.3* in the response of *M. truncatula* to N limitation in order to increase the ability of the plant to acquire this nutrient. This expression pattern is consistent with that of the ammonium transporter, *AtAMT1.1*, that is also up-regulated by N deficiency and down-regulated by addition of ammonium or nitrate (Yuan *et al.*, 2007; Lanquar *et al.*, 2009; Lanquar and Frommer, 2010). Similarly, several high-affinity phosphate transporters (*AtPT1* and *AtPT2*) were induced by Pi starvation and suggested to be involved in the alleviation of the stress (Karthikeyan *et al.*, 2002, 2007).

MtNRT1.3 *may play a role in* NO_3^- *sensing and regulation of primary root growth*

Several studies in *Arabidopsis* have demonstrated that the dual-affinity nitrate transporter AtNRT1.1 is not only

involved in root NO_3^- uptake but also has an important role in the regulation of the root architecture as part of the NO_3^--sensing pathway that mediates the stimulatory effect of NO_3^- on lateral root growth (Zhang and Forde, 1998; Zhang *et al.*, 1999; Remans *et al.*, 2006). This effect has been linked to the ability of AtNRT1.1 to mediate auxin transport in lateral roots depending on NO_3^- concentrations (Krouk *et al.*, 2010; Gojon *et al.*, 2011). It has been speculated that such a function may not be restricted to AtNRT1.1 and may concern other members of the PTR superfamily (Gojon *et al.*, 2011). An interesting candidate was found in *M. truncatula*. The *latd/nip* mutations affecting a NRT1(PTR) protein disrupt the organization of root meristems and result in the arrest of primary root development a few days after completion of germination (Liang *et al.*, 2007). In addition, *latd/nip* mutants were insensitive to the inhibitory effect of NO_3^- on primary root length (Yendrek *et al.*, 2010). Therefore, it was proposed that LATD/NIP might perceive the NO_3^- signal; however, transport activity has not yet been tested (Yendrek *et al.*, 2010). In the present work the coincidence of *MtNRT1.3* with the peak of a major QTL involved in the control of the variation of primary root growth, under both N-free and N-containing conditions suggests that MtNRT1.3 may be implicated in the control of this trait.

Acknowledgements

The authors are grateful to Dr Yi-Fang Tsay of Academia Sinica, Taiwan for the gift of recombinant plasmid containing the cDNA of AtNRT1.1. The authors wish to thank Professor Olaf Pongs, Institute for Neuronal Signal Transduction, Hamburg, Germany for the gift of the *Xenopus* expression vector, Dr Julia Buitink and Dr Beatrice Teulat-Merah for helpful discussions, and Dr Romain Berruyer for statistical analysis. This work was supported by the Genoplante 2010 QUALITYLEGSEED project (GPLA06036G) and the QUALISEM programme funded by Région Pays de Loire.

References

Almagro A, Lin SH, Tsay YF. 2008. Characterization of the Arabidopsis nitrate transporter NRT1.6 reveals a role of nitrate in early embryo development. *The Plant Cell* **20,** 3289–3299.

Barbulova A, Rogato A, D'Apuzzo E, Omrane S, Chiurazzi M. 2007. Differential effects of combined N sources on early steps of the Nod factor-dependent transduction pathway in *Lotus japonicus*. *Molecular Plant-Microbe Interactions* **20,** 994–1003.

Chiu CC, Lin CS, Hsia AP, Su RC, Lin HL, Tsay YF. 2004. Mutation of a nitrate transporter, AtNRT1:4, results in a reduced petiole nitrate content and altered leaf development. *Plant and Cell Physiology* **45,** 1139–1148.

Crespi M, Frugier F. 2008. De novo organ formation from differentiated cells: root nodule organogenesis. *Science Signaling* **1,** re11.

Forde BG. 2000. Nitrate transporters in plants: structure, function and regulation. *Biochimica et Biophysica Acta* **1465,** 219–235.

Glass AD, Shaff JE, Kochian LV. 1992. Studies of the uptake of nitrate in barley: IV. Electrophysiology. *Plant Physiology* **99,** 456–463.

Glevarec G, Bouton S, Jaspard E, Riou MT, Cliquet JB, Suzuki A, Limami AM. 2004. Respective roles of the glutamine synthetase/glutamate synthase cycle and glutamate dehydrogenase in ammonium and amino acid metabolism during germination and post-germinative growth in the model legume *Medicago truncatula*.. *Planta* **219,** 286–297.

Gojon A, Krouk G, Perrine-Walker F, Laugier E. 2011. Nitrate transceptor(s) in plants. *Journal of Experimental Botany* **62,** 2299–2308.

Gonzalez-Rizzo S, Crespi M, Frugier F. 2006. The *Medicago truncatula* CRE1 cytokinin receptor regulates lateral root development and early symbiotic interaction with *Sinorhizobium meliloti*. *The Plant Cell* **18,** 2680–2693.

Guo F, Wang R, Chen M, Crawford N. 2001. The Arabidopsis dual-affinity nitrate transporter gene AtNRT1.1 (CHL1) is activated and functions in nascent organ development during vegetative and reproductive growth. *The Plant Cell* **13,** 1761–1777.

Ho CH, Lin SH, Hu HC, Tsay YF. 2009. CHL1 functions as a nitrate sensor in plants. *Cell* **138,** 1184–1194.

Huang NC, Chiang CS, Crawford NM, Tsay YF. 1996. CHL1 encodes a component of the low-affinity nitrate uptake system in Arabidopsis and shows cell type-specific expression in roots. *The Plant Cell* **8,** 2183–2191.

Huang NC, Liu KH, Lo HJ, Tsay YF. 1999. Cloning and functional characterization of an Arabidopsis nitrate transporter gene that encodes a constitutive component of low-affinity uptake. *The Plant Cell* **11,** 1381–1392.

Huguet T, Ghérardi M, Chardon F, Sartorel EJP. 2007. Creation of consensus genetic–physical map (CGPM) for the identification of *Medicago truncatula* genes involved in natural populations. Abstracts of the Model Legume Congress, Tunis, Tunisia, 24–28 March.

Jeudy C, Ruffel S, Freixes S, *et al*. 2010. Adaptation of *Medicago truncatula* to nitrogen limitation is modulated via local and systemic nodule developmental responses. *New Phytologist* **185,** 817–828.

Jourjon MF, Jasson S, Marcel J, Ngom B, Mangin B. 2005. MCQTL: multi-allelic QTL mapping in multi-cross design. *Bioinformatics* **21,** 128–130.

Karthikeyan AS, Varadarajan DK, Jain A, Held MA, Carpita NC, Raghothama KG. 2007. Phosphate starvation responses are mediated by sugar signaling in Arabidopsis. *Planta* **225,** 907–918.

Karthikeyan AS, Varadarajan DK, Mukatira UT, D'Urzo MP, Damsz B, Raghothama KG. 2002. Regulated expression of Arabidopsis phosphate transporters. *Plant Physiology* **130,** 221–233.

Krouk G, Lacombe B, Bielach A, *et al*. 2010. Nitrate-regulated auxin transport by NRT1.1 defines a mechanism for nutrient sensing in plants. *Developmental Cell* **18,** 927–937.

Krusell L, Madsen LH, Sato S, *et al*. 2002. Shoot control of root development and nodulation is mediated by a receptor-like kinase. *Nature* **420,** 422–426.

Lanquar V, Frommer WB. 2010. Adjusting ammonium uptake via phosphorylation. *Plant Signaling and Behavior* **5,** 736–738.

Lanquar V, Loqué D, Hörmann F, Yuan L, Bohner A, Engelsberger WR, Lalonde S, Schulze WX, von Wirén N, Frommer WB. 2009. Feedback inhibition of ammonium uptake by a phospho-dependent allosteric mechanism in Arabidopsis. *The Plant Cell* **21,** 3610–3622.

Liang Y, Mitchell DM, Harris JM. 2007. Abscisic acid rescues the root meristem defects of the *Medicago truncatula* latd mutant. *Developmental Biology* **304,** 297–307.

Limami AM, Rouillon C, Glevarec G, Gallais A, Hirel B. 2002. Genetic and physiological analysis of germination efficiency in maize in relation to nitrogen metabolism reveals the importance of cytosolic glutamine synthetase. *Plant Physiology* **130,** 1860–1870.

Lin C, Koh S, Stacey G, Yu S, Lin T, Tsay Y. 2000. Cloning and functional characterization of a constitutively expressed nitrate transporter gene, OsNRT1, from rice. *Plant Physiology* **122,** 379–388.

Lin SH, Kuo HF, Canivenc G, *et al*. 2008. Mutation of the Arabidopsis NRT1.5 nitrate transporter causes defective root-to-shoot nitrate transport. *The Plant Cell* **20,** 2514–2528.

Liu KH, Huang CY, Tsay YF. 1999. CHL1 is a dual-affinity nitrate transporter of Arabidopsis involved in multiple phases of nitrate uptake. *The Plant Cell* **11,** 865–874.

Liu K, Tsay Y. 2003. Switching between the two action modes of the dual-affinity nitrate transporter CHL1 by phosphorylation. *EMBO Journal* **22,** 1005–1013.

Miller AJ, Fan X, Orsel M, Smith SJ, Wells DM. 2007. Nitrate transport and signalling. *Journal of Experimental Botany* **58,** 2297–2306.

Nishimura R, Hayashi M, Wu GJ, *et al*. 2002. HAR1 mediates systemic regulation of symbiotic organ development. *Nature* **420,** 426–429.

Okamoto S, Ohnishi E, Sato S, Takahashi H, Nakazono M, Tabata S, Kawaguchi M. 2009. Nod factor/nitrate-induced CLE genes that drive HAR1-mediated systemic regulation of nodulation. *Plant and Cell Physiology* **50,** 67–77.

Omrane S, Ferrarini A, D'Apuzzo E, Rogato A, Delledonne M, Chiurazzi M. 2009. Symbiotic competence in *Lotus japonicus* is affected by plant nitrogen status: transcriptomic identification of genes affected by a new signalling pathway. *New Phytologist* **183,** 380–394.

Pierre JB, Huguet T, Barre P, Huyghe C, Julier B. 2008. Detection of QTLs for flowering date in three mapping populations of the model legume species *Medicago truncatula*. *Theoretical and Applied Genetics* **117,** 609–620.

Remans T, Nacry P, Pervent M, Filleur S, Diatloff E, Mounier E, Tillard P, Forde BG, Gojon A. 2006. The Arabidopsis NRT1.1 transporter participates in the signaling pathway triggering root colonization of nitrate-rich patches. *Proceedings of the National Academy of Sciences, USA* **103,** 19206–19211.

Richard-Molard C, Wuilleme S, Scheel C, Gresshoff PM, Morot-Gaudry JF, Limami AM. 1999. Nitrogen-induced changes in morphological development and bacterial susceptibility of Belgian endive (*Cichorium intybus* L.) are genotype-dependent. *Planta* **209,** 389–398.

Ruffel S, Freixes S, Balzergue S, *et al*. 2008. Systemic signaling of the plant nitrogen status triggers specific transcriptome responses depending on the nitrogen source in *Medicago truncatula*. *Plant Physiology* **146,** 2020–2035.

Schnabel E, Journet EP, de Carvalho-Niebel F, Duc G, Frugoli J. 2005. The *Medicago truncatula* SUNN gene encodes a CLV1-like leucine-rich repeat receptor kinase that regulates nodule number and root length. *Plant Molecular Biology* **58,** 809–822.

Searle IR, Men AE, Laniya TS, Buzas DM, Iturbe-Ormaetxe I, Carroll BJ, Gresshoff PM. 2003. Long-distance signaling in nodulation directed by a CLAVATA1-like receptor kinase. *Science* **299,** 109–112.

Segonzac C, Boyer JC, Ipotesi E, Szponarski W, Tillard P, Touraine B, Sommerer N, Rossignol M, Gibrat R. 2007. Nitrate efflux at the root plasma membrane: identification of an Arabidopsis excretion transporter. *The Plant Cell* **19,** 3760–3777.

Shih T, Smith R, Toro L, Goldin A. 1998. High-level expression and detection of ion channels in Xenopus oocytes. *Methods in Enzymology* **293,** 529–556.

Siddiqi MY, Glass AD, Ruth TJ, Fernando M. 1989. Studies of the regulation of nitrate influx by barley seedlings using NO(3). *Plant Physiology* **90,** 806–813.

Siddiqi MY, Glass AD, Ruth TJ, Rufty TW. 1990. Studies of the uptake of nitrate in barley: I. Kinetics of NO(3) influx. *Plant Physiology* **93,** 1426–1432.

Streeter JG. 1985*a*. Nitrate inhibition of legume nodule growth and activity: I. Long term studies with a continuous supply of nitrate. *Plant Physiology* **77,** 321–324.

Streeter JG. 1985*b*. Nitrate inhibition of legume nodule growth and activity: II. Short term studies with high nitrate supply. *Plant Physiology* **77,** 325–328.

Tsay YF, Chiu CC, Tsai CB, Ho CH, Hsu PK. 2007. Nitrate transporters and peptide transporters. *FEBS Letters* **581,** 2290–2300.

Tsay YF, Schroeder JI, Feldmann KA, Crawford NM. 1993. The herbicide sensitivity gene CHL1 of Arabidopsis encodes a nitrate-inducible nitrate transporter. *Cell* **72,** 705–713.

Vandecasteele C, Teulat-Merah B, Morère-Le Paven MC, *et al*. 2011. QTL analysis reveals a correlation between the ratio of sucrose/raffinose family oligosaccharides and seed vigour in *Medicago truncatula*. *Plant, Cell and Environment* (in press).

Walch-Liu P, Forde BG. 2008. Nitrate signalling mediated by the NRT1.1 nitrate transporter antagonises l-glutamate-induced changes in root architecture. *The Plant Journal* **54,** 820–828.

Walch-Liu P, Liu LH, Remans T, Tester M, Forde BG. 2006. Evidence that l-glutamate can act as an exogenous signal to modulate root growth and branching in *Arabidopsis thaliana*. *Plant and Cell Physiology* **47,** 1045–1057.

Wang R, Liu D, Crawford N. 1998. The Arabidopsis CHL1 protein plays a major role in high-affinity nitrate uptake. *Proceedings of the National Academy of Sciences, USA* **95,** 15134–15139.

Yendrek CR, Lee YC, Morris V, *et al*. 2010. A putative transporter is essential for integrating nutrient and hormone signaling with lateral root growth and nodule development in *Medicago truncatula*. *The Plant Journal* **62,** 100–112.

Yokoyama T, Kodama N, Aoshima H, Izu H, Matsushita K, Yamada M. 2001. Cloning of a cDNA for a constitutive NRT1 transporter from soybean and comparison of gene expression of soybean NRT1 transporters. *Biochimica et Biophysica Acta* **1518,** 79–86.

Yuan L, Loqué D, Ye F, Frommer WB, von Wirén N. 2007. Nitrogen-dependent posttranscriptional regulation of the ammonium transporter AtAMT1;1. *Plant Physiology* **143,** 732–744.

Zhang H, Forde BG. 1998. An Arabidopsis MADS box gene that controls nutrient-induced changes in root architecture. *Science* **279,** 407–409.

Zhang H, Jennings A, Barlow PW, Forde BG. 1999. Dual pathways for regulation of root branching by nitrate. *Proceedings of the National Academy of Sciences, USA* **96,** 6529–6534.

Zhou J, Theodoulou F, Muldin I, Ingemarsson B, Miller A. 1998. Cloning and functional characterization of a *Brassica napus* transporter that is able to transport nitrate and histidine. *Journal of Biological Chemistry* **273,** 12017–12023.

Zifarelli G, Pusch M. 2010. CLC transport proteins in plants. *FEBS Letters* **584,** 2122–2127.